acta physica slovaca vol. 48 No. 2, 67 – 76 April 1998

SENSITIVITY OF RIA PROTON–NUCLEUS ELASTIC SCATTERING CALCULATIONS ON RMF PARAMETERIZATIONS

M. Hojsík†, **Š. Gmuca**‡1

†*Faculty of Mathematics and Physics, Comenius University, Mlynská dolina, Bratislava, Slovakia*

‡*Institute of Physics, Slovak Academy of Sciences, Dúbravska cesta, Bratislava, Slovakia*

Relativistic microscopic calculations are presented for proton elastic scattering from ^{40}Ca at 500 MeV. The underlying target densities are calculated within the framework of the relativistic mean–field theory with several parameter sets commonly in use. The selfconsistency of the scalar and vector densities is preserved. The sensitivity of the scattering observables to nuclear densities (and thus to relativistic mean–field parameters) is investigated.

Received 15 January 1998, in final form 16 February 1998, accepted 18 February 1998

1. Introduction

Recently, the relativistic impulse approximation (RIA) [1, 2] has been widely and repeatedly used for the calculations of proton–nucleus scattering at intermediate energies. These calculations have exhibited significant improvements over the nonrelativistic approaches. The RIA calculations, in particular, provide a dramatically better description of the spin observables, namely the analyzing power, A_y, and the spin–rotation function, Q, at least for energies higher than 400 MeV [3].

In the RIA, the Dirac optical potential is obtained by folding of the local NN Lorentz–invariant amplitudes with the corresponding nuclear densities. For the spin–zero targets the scalar and vector terms give the dominant contributions. Thus the scalar and vector nuclear densities (both, proton and neutron ones) play the dominant role in the RIA calculations.

While the proton vector densities can be obtained by unfolding from the empirically known charge densities [4], all other densities used rely to a great extent on theoretical models. The various recipes are used to construct the neutron vector densities and the scalar densities for both, neutrons and protons.

In this paper we will study the sensitivity of the RIA results on the various sets of relativistic mean–field (RMF) parameters currently in use. Different sets of RMF parameters produce slightly different densities which (when used in the RIA calculations)

1 E-mail address: gmuca@savba.sk

0323-0465/98

give different predictions for the nucleon–nucleus scattering observables. This enables us to study a sensitivity of the RIA calculations to the RMF parameterizations.

This paper is organized as follows. In Sec. 2 we outline the theoretical background of the RIA and RMF models. Sec. 3 is devoted to calculations of the proton scattering observables on the ^{40}Ca nucleus at 500 MeV. The results are compared with experimental data. Finally, in Sec. 4 we present a summary and draw conclusions from this work.

2. Theoretical models

2.1. Relativistic impulse approximation

Applications of Dirac phenomenology to proton scattering on nuclei [5, 6, 7] clearly indicated its ability to describe experimental data over a wide range of energy. Analyses at intermediate energies using a Dirac equation with Lorentz scalar and Lorentz four–vector (time–like component only) complex optical potentials have proven superior to the nonrelativistic treatment, especially with regard to spin observables.

The Dirac equation for proton scattering may be written as

$$\{\boldsymbol{\alpha}.\boldsymbol{p} + \beta\,[m + U_S(\boldsymbol{r})] + [U_0(\boldsymbol{r}) + V_C(\boldsymbol{r})]\}\,\psi(\boldsymbol{r}) = E\psi(\boldsymbol{r}), \tag{1}$$

where U_S and U_0 are the scalar and vector potentials, respectively, V_C is the Coulomb potential, E is the c.m. energy of the impinging proton and m is its mass. In Dirac phenomenology the optical potentials are obtained by a fit of prescribed functional forms to elastic proton scattering data.

Contrary to the Dirac phenomenology, the relativistic impulse approximation (RIA) [1, 2] offers a parameter–free approach to the proton scattering at intermediate energies. The RIA is based on an assumption that the NN interaction between the projectile and target is unmodified by the surrounding nucleons. This assumption is valid at high energies, while at lower energies the important corrections from Pauli blocking and exchange contributions [8] have to be accounted for.

The RIA consists of the use of the experimental NN scattering amplitudes. The constraints of Lorentz covariance, parity conservation, isospin invariance and that free nucleons are on their mass shell imply that the invariant NN scattering operator $\mathcal{F}$ can be written in terms of five complex functions (one set for pp scattering and one set for pn scattering).

$$\mathcal{F}(q) = \mathcal{F}_S + \mathcal{F}_V\gamma_1^{\mu}\gamma_{2\mu} + \mathcal{F}_P\gamma_1^5\gamma_2^5 + \mathcal{F}_A\gamma_1^5\gamma_1^{\mu}\gamma_2^5\gamma_{2\mu} + \mathcal{F}_T\sigma_1^{\mu\nu}\sigma_{2\mu\nu} \tag{2}$$

For spin–saturated spherical target nuclei the largest contributions arise from the scalar and vector terms ($\mathcal{F}_S$ and $\mathcal{F}_V$, respectively); the tensor term ($\mathcal{F}_T$) is small and is usually neglected, while the pseudoscalar ($\mathcal{F}_P$) and axial vector ($\mathcal{F}_A$) terms doesn't contribute. Thus for these nuclei the RIA Dirac optical potential is (in momentum space)

$$U_{\rm opt}(q) = -\frac{4\pi i k}{m}\left[\mathcal{F}_S(q)\rho_S(q) + \gamma^0\mathcal{F}_V(q)\rho_V(q)\right], \tag{3}$$

where k is the proton–nucleus center–of–mass (c.m.) wave number, q is the momentum transfer, ρ_S and ρ_V are the scalar and vector densities, respectively, and $\mathcal{F}_S$ and $\mathcal{F}_V$ are the scalar and vector NN invariant amplitudes.

The Dirac optical potential in coordinate space is then obtained by the Fourier transform of $U_{\rm opt}(q)$. This yields the scalar and vector RIA potentials to be used in the Dirac equation.

2.2. Relativistic mean–field approach

To evaluate the RIA Dirac optical potential one needs the scalar and vector densities for both, protons and neutrons. The convenient tool to obtain them presents the relativistic mean field (RMF) theory [9]. The RMF model is now a standard approach in nuclear physics. For completeness we write essentials of the underlying theory (for more details see e.g. [10]).

Our starting point is the Lagrangian density which includes the baryon field (ψ), neutral scalar and vector meson fields (σ, ω), the isovector $\boldsymbol{\rho}$ meson field together with an electromagnetic interaction. In addition, the cubic and quartic self–interactions of the scalar meson field and the quartic self–coupling of the vector meson field have been added to allow the model enough flexibility in describing nuclear properties.

The full Lagrangian density reads

$$\begin{aligned}\mathcal{L} \;=\; & \overline{\psi}(i\gamma_\mu\partial^\mu - M)\psi \\ & + \frac{1}{2}\partial_\mu\sigma\partial^\mu\sigma - \frac{1}{2}m_\sigma^2\sigma^2 - \frac{1}{3}b_\sigma M(g_\sigma\sigma)^3 - \frac{1}{4}c_\sigma(g_\sigma\sigma)^4 - g_\sigma\overline{\psi}\psi\sigma \\ & - \frac{1}{4}\omega_{\mu\nu}\omega^{\mu\nu} + \frac{1}{2}m_\omega^2\omega_\mu\omega^\mu + \frac{1}{4}c_\omega(g_\omega^2\omega_\mu\omega^\mu)^2 - g_\omega\overline{\psi}\gamma_\mu\psi\omega^\mu \\ & - \frac{1}{4}\boldsymbol{\rho}_{\mu\nu}\boldsymbol{\rho}^{\mu\nu} + \frac{1}{2}m_\rho^2\boldsymbol{\rho}_\mu\boldsymbol{\rho}^\mu - g_\rho\overline{\psi}\gamma_\mu\boldsymbol{\tau}\psi\boldsymbol{\rho}^\mu \\ & - \frac{1}{4}F_{\mu\nu}F^{\mu\nu} - e\overline{\psi}\gamma_\mu\frac{(1-\tau_3)}{2}\psi A^\mu,\end{aligned} \tag{4}$$

where the symbols used have their usual meaning [9, 10].

The Lagrangian given above is treated in the mean–field approximation; i.e. the meson fields are not quantized, but are replaced by their expectation values which are the condensed classical fields. The equations of motion are then obtained from the Lagrangian by the standard technique of field variation. The Euler–Lagrange equations provide a Dirac equation for the nucleon and Klein–Gordon equations for the meson fields.

The static solution for the nucleon field is obtained by solving the stationary Dirac equation

$$\{-i\boldsymbol{\alpha}\cdot\boldsymbol{\nabla} + \beta\,[M + S(\boldsymbol{r})] + V(\boldsymbol{r})\}\,\psi_i(\boldsymbol{r}) = \epsilon_i\psi_i(\boldsymbol{r}), \tag{5}$$

where the scalar potential is given by

$$S(\boldsymbol{r}) = g_\sigma\sigma(\boldsymbol{r}), \tag{6}$$

while the vector potential has more complicated structure

$$V(r) = g_\omega \omega^0(r) + g_\rho \tau_3 \rho^0(r) + e\frac{(1-\tau_3)}{2}A^0(r). \tag{7}$$

The vector potential V(r) contains only a time-like component. The spatial currents vanish due to the requirement of spherical symmetry. Charge conservation guarantees that only the third isotopic component of ρ survives.

The Klein–Gordon equations for the meson and the electromagnetic fields are

$$\begin{aligned}
(-\Delta + m_\sigma^2)\,\sigma(r) &= -g_\sigma \left\{\rho_S(r) + b_\sigma M\,[g_\sigma\sigma(r)]^2 + c_\sigma\,[g_\sigma\sigma(r)]^3\right\}, && (8)\\
(-\Delta + m_\omega^2)\,\omega^0(r) &= g_\omega \left\{\rho_V(r) - c_\omega\,[g_\omega\omega^0(r)]^3\right\}, && (9)\\
(-\Delta + m_\rho^2)\,\rho^0(r) &= g_\rho \rho_3(r), && (10)\\
-\Delta A^0(r) &= e\rho_V^{(p)}(r), && (11)
\end{aligned}$$

where the sources are determined by the corresponding densities in the static nucleus. Namely,

$$\begin{aligned}
\rho_S(r) &= \sum_\alpha^{occ.} \overline{\psi}_\alpha(r)\psi_\alpha(r), && (12)\\
\rho_V(r) &= \sum_\alpha^{occ.} \psi_\alpha^\dagger(r)\psi_\alpha(r), && (13)\\
\rho_3(r) &= \sum_\alpha^{occ.} \psi_\alpha^\dagger(r)\tau_3\psi_\alpha(r), && (14)\\
\rho_V^{(p)}(r) &= \sum_\alpha^{occ.} \psi_\alpha^\dagger(r)\frac{(1-\tau_3)}{2}\psi_\alpha(r). && (15)
\end{aligned}$$

(16)

Here the sums are taken over the occupied particle states only. This implies that the contributions from negative-energy states are neglected (*no-sea* approximation), i.e. the vacuum is not polarized.

The above set of equations are to be solved iteratively. One starts with an initial guess of the fields (e.g. in the form of Woods-Saxon potentials). The Dirac equation is then solved with these potential terms to yield the nucleon spinors which are subsequently used to obtain the new sources (densities). The meson and photon equations are then solved with these sources to get a new set of fields to be used for the calculation of new potential terms. The Dirac equation is then solved again with the new potentials to get the spinors to be used to obtain the new sources for the meson fields. This iterative procedure is continued until the selfconsistency conditions are achieved.

3. Results

The microscopic description of nucleon elastic scattering from nuclei using RIA requires the calculation of the nucleon densities in the target. The RIA optical potential employs the scalar and vector densities for both protons and neutrons (the tensor terms are small and were omitted). With the exception of the proton-vector density (which, in principle, can be obtained by unfolding the single proton form factor from the nuclear charge density) all of these rely on the theoretical models of nuclear structure.

In the present work we have calculated all nuclear densities using the RMF model with various parameter sets. It is the aim of this work to study the sensitivity of the RIA results on the parameter set used.

In most of the previous RIA studies (see e.g. [3, 11]) the proton-vector densities were obtained by unfolding the single proton electric form factor from the nuclear charge densities, while the neutron-vector densities were taken as

$$\rho_V^n(r) = \rho_V^p + [\rho_V^n(r) - \rho_V^p(r)]_{TH}, \tag{17}$$

where the neutron and proton densities in the square brackets are some theoretical mean-field calculations, either nonrelativistic (e.g. Hartree-Fock-Bogoliubov (HFB) distributions of Dechargé and Gogny [12]), or relativistic ones (e.g. [13]).

Similarly, the scalar densities were constructed according to the prescription

$$\rho_S^{n(p)}(r) = \rho_V^{n(p)} + [\rho_S^{n(p)}(r) - \rho_V^{n(p)}(r)]_{RMF}, \tag{18}$$

where square brackets denote the results of some RMF calculations.

It is clear that by using such recipes the selfconsistent relationship between the scalar and vector densities is lost. However, we believe it is important to retain this selfconsistency, as the scalar density is not an observable. It is the pure relativistic quantity having no nonrelativistic counterpart, and we have only indirect information on its behaviour.

In this introductory paper we present the results for the p+^{40}Ca elastic scattering at 500 MeV. The ^{40}Ca nucleus is of doubly-magic character and was included in all set-of-nuclei used in the procedures for obtaining the RMF parameters [14]. The current RMF parameter sets in use describe the ground-state properties (charge density, charge radius, binding energy, ...) of the ^{40}Ca nucleus pretty well and, therefore, it is of interest to see how the minor deviations in densities (scalar-vector, proton-neutron) produced by various RMF parameters propagate into the differences of the RIA predictions of elastic scattering observables. In the subsequent paper we will study these differences for several nuclei and several incident energies.

We have calculated the ^{40}Ca densities using the RMF model with the NL1 [15], NL2 [16], NL-SH [17] and TM1 [18] parameters. The values of the parameter sets used are listed in Table 1.

The NL1 parameter set was obtained by fitting the total binding energies, the diffraction radii and the surface thickness for some doubly-magic or semi-magic nuclei along the stability line. It provides a good description of binding energies and charge radii for most of stable nuclei. However, for nuclei away from the stability line the results

Table 1. The RMF parameter sets used in the present study.

	NL1 Ref. [15]	NL2 Ref. [16]	NL–SH Ref. [17]	TM1 Ref. [18]
M (MeV)	938.0	938.0	939.0	938.0
m_σ (MeV)	492.25	504.89	526.059	511.198
m_ω (MeV)	795.36	780.0	783.0	783.0
m_ρ (MeV)	763.0	763.0	763.0	770.0
g_σ^2	102.77310	83.01433	109.07714	100.57884
g_ω^2	176.49123	132.08445	167.57561	159.11047
g_ρ^2	24.75560	29.01546	19.20894	21.45728
b_σ	0.0024578	0.0006408	0.0012748	0.0015083
c_σ	-0.0034344	0.0020002	-0.0013310	0.0000611
c_ω	–	–	–	0.0028166

are less satisfactory, probably due to the large asymmetry energy ~44 MeV. The NL2 parameters were obtained similarly as the NL1, however, with a constraint for a smaller spin–orbit splittings.

For the NL–SH set the charge radii were used instead of the diffraction radii and the neutron radii were added to treat the isospin asymmetry in a better way. This resulted in a remarkably successful parameter set with an improved isovector properties and an asymmetry energy of ~36 MeV. NL–SH was extensively applied throughout the chart of nuclides including neutron–rich nuclei and superheavy elements [19].

TM1 parameter set differs from the previous ones by incorporating the quartic self–interaction of the vector–isoscalar ω field, as suggested by Bodmer [20] and Gmuca [21]. This term casts the density dependence into the vector potential, an effect originating from relativistic Brueckner–Hartree–Fock calculations of nuclear matter [22].

In Fig. 1 we can compare the experimental and calculated charge densities of the ^{40}Ca nucleus. The results indicate differences in charge densities produced by various RMF parameters. The NL1 parameter set treats correctly the nuclear surface and slightly overestimates the empirical charge density at the centre of the nucleus. The remaining three parameter sets produce rather similar results which behave better in the nuclear interior, however, fall down more steeply at the nuclear surface (thus giving smaller charge radius). Similar results one may obtain also for the point scalar and vector densities for both, protons and neutrons.

Comparing the RIA results obtained with densities calculated by various RMF parameters allows us to study the sensitivity of the scattering observables to these parameter sets.

Figure 2 shows the results of the RIA calculations for an angular distributions of the elastic scattering cross section. The experimental data points are from [23]. The curves represent the results for various RMF parameters used. We can observe that differences among RMF parameter sets became significant for angles greater than 16°. For an increasing angle this difference becomes yet greater. The sensitivity of the cross

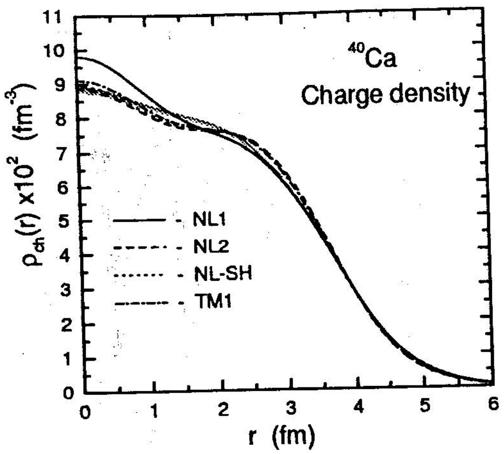

Fig. 1. Comparison of experimental charge density of ^{40}Ca (gray area) to RMF calculations (labels indicate the RMF parameters used).

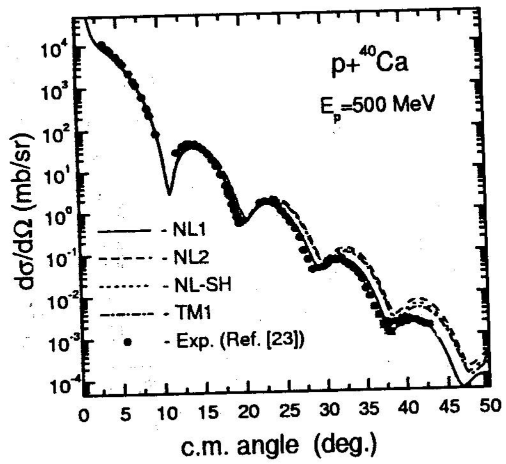

Fig. 2. Sensitivity of the proton elastic scattering cross section to the RMF parameters. The shaded area represents the band of RIA predictions using the ^{40}Ca ground state densities as calculated by the RMF approach with the various parameter sets (labels indicate the RMF parameter set used - see text). The experimental data (points) are from Ref.[23].

section prediction on the RMF parameters is rather high. The detailed inspection of the figure gives some preference to thr NL1 [15] parameter set among the RMF parameters used, as it clearly describes the differential cross section more correctly than others.

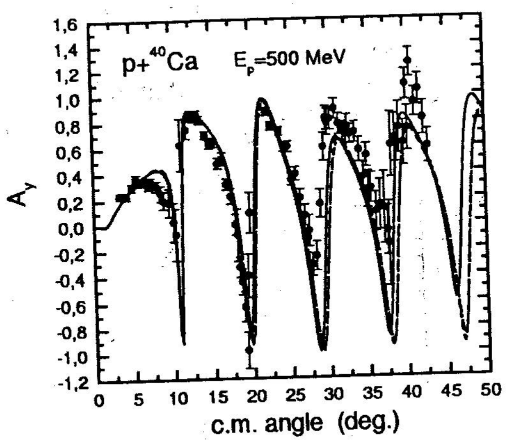

Fig. 3. The same as in Fig. 2, except for the analyzing power, A_y.

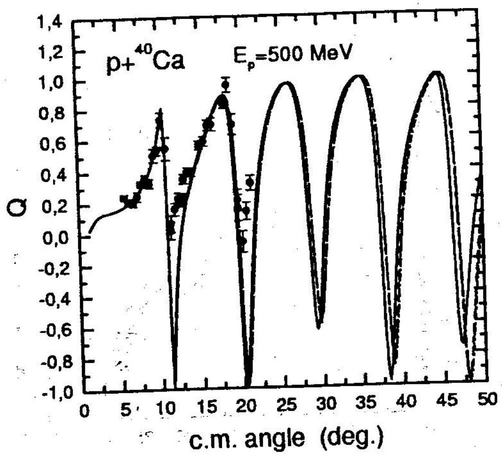

Fig. 4. The same as in Fig. 2, except for the spin–rotation function, Q. The experimental data (points) are from Ref.[24].

Figures 3 and 4 show the results obtained for an analyzing power A_y and spin–rotation function Q, respectively. The experimental data for A_y are taken from [23], and those for Q from [24]. The calculations follow the structure of experimental data remarkably well and produce a narrow band of allowable predictions, none of which can be excluded. This indicate that spin dynamics is inherent in the relativistic formalism and arises naturally from the large Lorentz scalar and vector potentials in the Dirac

equation. The sensitivity of the spin observables on the RMF parameter set is weak.

4. Conclusions

We have studied the sensitivity of the RIA scattering predictions on the RMF parameters for the p+^{40}Ca elastic scattering at 500 MeV. The various RMF parameter sets were used to get the ground state densities. Using them in the RIA calculations, the minor differences among the densities propagate into the different RIA predictions for the proton–nucleus scattering observables. It is important that in the present approach the selfconsistent relationship between scalar and vector densities is preserved.

We have shown that there is a little sensitivity in the spin scattering observables, the analyzing power, A_y, and spin-rotation function, Q. This demonstrate that a correct description of the spin dynamics is an inherent property of the relativistic approaches. Since the structure of A_y and Q predictions by RIA are known to be acutely sensitive to the scalar–vector density difference [3], this further confirms the necessity of the selfconsistency condition on the scalar–vector density relation (i.e., lower components of the relativistic target wave functions).

On the other hand, the sensitivity of the angular distribution of the elastic scattering cross section prediction on the RMF parameters is rather high. All the RMF parameter sets used describe the charge density (i.e., mainly the proton density) of the ^{40}Ca nucleus almost equally well, thus this sensitivity may be due to the differences in the neutron–vector densities. This conclusion will be further tested in the next paper. If being confirmed, the RIA predictions of the proton elastic scattering observable may became valuable constraints upon choosing the most appropriate RMF parameters.

Acknowledgements This work was supported in part by the VEGA agency under grant no. 95/5305/645.

References

[1] J.A. McNeil, J.R. Shepard and S.J. Wallace: *Phys. Rev. Lett.* **50** (1983) 1439
[2] J.R. Shepard, J.A. McNeil and S.J. Wallace: *Phys. Rev. Lett.* **50** (1983) 1443
[3] L. Ray and G.W. Hoffmann: *Phys. Rev.* **C 31** (1985) 538
[4] H. deVries, C.W. deJager and C. deVries: *At. Data Nucl. Data Tables* **36** (1987) 495
[5] L.G. Arnold, B.C. Clark, R.L. Mercer and P. Schwandt: *Phys. Rev.* **C 23** (1981) 1949
[6] B.C. Clark, S. Hama and R.L. Mercer: *in AIP Conf. Proc No. 97* ed. H.O. Meyer (AIP, New York, 1982), p.260
[7] B.C. Clark, R.L. Mercer and P. Schwandt: *Phys. Lett.* **122B** (1983) 211
[8] D.P. Murdock and C.J. Horowitz: *Phys. Rev.* **C 35** (1987) 1442
[9] B.D. Serot and J.D. Walecka: *Adv. Nucl. Phys.* **16** (1986) 1
[10] Y.K. Gambhir, P. Ring and A. Thimet: *Ann. Phys. N.Y.* **198** (1990) 132
[11] W. Rory Coker and L. Ray: *Phys. Rev.* **C 42** (1990) 659
[12] J. Dechargé and D. Gogny: *Phys. Rev.* **C 21** (1980) 1568
[13] C.J. Horowitz and B.D. Serot: *Nucl. Phys.* **A368** (1981) 503

[14] P.-G. Reinhard: *Rep. Prog. Phys.* **52** (1989) 439

[15] P.-G. Reinhard, M. Rufa, J. Maruhn, W. Greiner and J. Friedrich: *Z. Phys.* **A 323** (1986) 13

[16] S.J. Lee, J. Fink, A.B. Balantekin, M. Strayer, A.S. Umar, P.-G. Reinhard, J.A. Maruhn and W. Greiner: *Phys. Rev. Lett.* **57** (1986) 2916

[17] M.M. Sharma, M.A. Nagarajan and P. Ring: *Phys. Lett.* **B 312** (1993) 377

[18] Y. Sugahara and H. Toki: *Nucl. Phys.* **A 579** (1994) 557

[19] G.A. Lalazissis, M.M. Sharma, P. Ring and Y.K Gambhir: *Nucl. Phys.* **A 608** (1996) 202

[20] A.R. Bodmer: *Nucl. Phys.* **A 526** (1991) 903

[21] S. Gmuca: *Nucl. Phys.* **A 547** (1992) 447
S. Gmuca: *Z. Phys.* **A 342** (1992) 387

[22] R. Brockmann and R. Machleidt: *Phys. Rev.* **C 42** (1990) 1965

[23] D.A. Hutcheon *et al.*: *Nucl. Phys.* **A 483** (1988) 429

[24] B. Aas *et al.*: *Nucl. Phys.* **A 460** (1986) 675